



ATTI  
DELLA  
SOCIETÀ TOSCANA  
DI  
SCIENZE NATURALI

MEMORIE • SERIE A • VOLUME CXXVI • ANNO 2019



Edizioni ETS



## INDICE - CONTENTS

- P. FULIGNATI, P. MARIANELLI, A. SBRANA – Quantitative SEM-EDS analysis of reference silicate mineral and glass samples.  
*Analisi quantitative SEM-EDS di campioni di riferimento di vetri e minerali silicatici.* pag. 5
- G. GALLELLO, J. BERNABEU, A. DIEZ-CASTILLO, P. ESCRIBA, A. PASTOR, M. LEZZERINI, S. CHENERY, M.E. HODSON, D. STUMP – Developing REE parameters for soil and sediment profile analysis to identify Neolithic anthropogenic signatures at Serpis Valley (Spain).  
*Sviluppo di parametri REE per l'analisi del profilo del suolo e dei sedimenti per identificare le firme antropogeniche neolitiche nella valle del Serpis (Spagna).* » 13
- D. MAURO, C. BIAGIONI, M. PASERO, H. SKOGBY – Crystal-chemistry of sulfates from the Apuan Alps (Tuscany, Italy). III. Mg-rich sulfate assemblages from the Fornovolasco mining complex.  
*Cristallochimica dei solfati delle Alpi Apuane (Toscana, Italia). III. Associazioni a solfati ricchi in Mg dal complesso minerario di Fornovolasco.* » 33
- P. ORLANDI, M. D'ORAZIO – Cinnabar and other high-density minerals from stream sediments of Monti Pisani (Pisa and Lucca provinces, Tuscany).  
*Cinabro ed altri minerali ad elevata densità negli "stream sediments" dei Monti Pisani (Province di Lucca e Pisa, Toscana).* » 45
- M. BACCI, S. CORSI, L. LOMBARDI, M. GIUNTI – Gli interventi di ripristino morfologico ed ecologico del sistema dunale del Golfo di Follonica (Toscana, Italia): tecniche utilizzate e risultati del monitoraggio.  
*Morphological and ecological activities to restore the dune system at the Follonica Gulf (Tuscany, Italy): techniques used and monitoring results.* » 57
- D. MAGALDI – Interglacial Pleistocene paleosols supporting old roads in central Tuscany.  
*Paleosuoli del Pleistocene interglaciale a supporto di antiche strade nella Toscana centrale.* » 67
- V. SPADINI – Pliocene scleractinians from Estepona (Malaga, Spain).  
*Sclerattiniani pliocenici di Estepona (Malaga, Spagna).* » 75
- R. GIANNECCHINI, M. AMBROSIO, A. DEL SORDO, M.T. FAGIOLI, A. SARTELLI, Y. GALANTI – Hydrogeological numerical modeling of the southeastern portion of the Lucca Plain (Tuscany, Italy), stressed by groundwater exploitation.  
*Modello idrogeologico numerico del settore sud-orientale della Piana di Lucca (Toscana, Italia) caratterizzato da sfruttamento intensivo delle risorse idriche.* » 95
- W. LANDINI – In memoria di Marco Tongiorgi (1934-2019).  
*In memory of Marco Tongiorgi (1934-2019).* » 111
- Processi Verbali della Società Toscana di Scienza Naturale residente in Pisa. Anno 2019 - <http://www.stsn.it>. » 121



DANIELA MAURO <sup>(1)</sup>, CRISTIAN BIAGIONI <sup>(1)</sup>, MARCO PASERO <sup>(1)</sup>, HENRIK SKOGBY <sup>(2)</sup>

## CRYSTAL-CHEMISTRY OF SULFATES FROM THE APUAN ALPS (TUSCANY, ITALY). III. Mg-RICH SULFATE ASSEMBLAGES FROM THE FORNOVOLASCO MINING COMPLEX

**Abstract** - D. MAURO, C. BIAGIONI, M. PASERO, H. SKOGBY, *Crystal-chemistry of sulfates from the Apuan Alps (Tuscany, Italy). III. Mg-rich sulfate assemblages from the Fornovolasco mining complex.*

A suite of sulfates from the Fornovolasco mine has been characterized through X-ray diffraction, chemical analyses, micro-Raman and FTIR spectroscopies. Four different mineral species have been identified: epsomite, halotrichite/pickeringite, magnesiocopiapite, and wilcoxite. Epsomite and wilcoxite were collected in samples suitable for single-crystal X-ray diffraction studies. Epsomite is orthorhombic, space group  $P2_12_12_1$ , with unit-cell parameters  $a = 11.8664(3)$ ,  $b = 12.0150(3)$ ,  $c = 6.8598(2)$  Å,  $V = 978.03(4)$  Å<sup>3</sup>. Wilcoxite is triclinic, space group  $P\bar{1}$ , with unit-cell parameters  $a = 6.6749(4)$ ,  $b = 6.7730(4)$ ,  $c = 14.9076(9)$  Å,  $\alpha = 79.604(3)$ ,  $\beta = 80.163(3)$ ,  $\gamma = 62.475(3)^\circ$ ,  $V = 584.90(6)$  Å<sup>3</sup>. The crystal structures of epsomite and wilcoxite have been refined to  $R_1 = 0.0207$  [for 3418 unique reflections with  $F_o > 4\sigma(F_o)$ ] and 176 refined parameters] and 0.0308 [for 3074 unique reflections with  $F_o > 4\sigma(F_o)$ ] and 216 refined parameters], respectively. These new data improve the knowledge about the secondary assemblages formed through the pyrite oxidation and allow a better understanding of the H-bond system in wilcoxite.

**Key words** - epsomite, wilcoxite, sulfate, crystal structure, hydrogen bonds, Fornovolasco, Apuan Alps

**Riassunto** - D. MAURO, C. BIAGIONI, M. PASERO, H. SKOGBY, *Cristallochimica dei solfati delle Alpi Apuane (Toscana, Italia). III. Associazioni a solfati ricchi in Mg dal complesso minerario di Fornovolasco.*

Una serie di campioni di solfati provenienti dalla miniera di Fornovolasco sono stati caratterizzati attraverso la diffrazione di raggi X, analisi chimiche e spettroscopie micro-Raman e FTIR. Sono state identificate quattro differenti specie mineralogiche: epsomite, alotrichite/pickeringite, magnesiocopiapite e wilcoxite. Epsomite e wilcoxite sono state raccolte in campioni utilizzabili per studi diffrattometrici con tecniche di cristallo singolo. L'epsomite è ortorombica, gruppo spaziale  $P2_12_12_1$ , con parametri di cella  $a = 11.8664(3)$ ,  $b = 12.0150(3)$ ,  $c = 6.8598(2)$  Å,  $V = 978.03(4)$  Å<sup>3</sup>. La wilcoxite è triclina, gruppo spaziale  $P\bar{1}$ , con parametri di cella  $a = 6.6749(4)$ ,  $b = 6.7730(4)$ ,  $c = 14.9076(9)$  Å,  $\alpha = 79.604(3)$ ,  $\beta = 80.163(3)$ ,  $\gamma = 62.475(3)^\circ$ ,  $V = 584.90(6)$  Å<sup>3</sup>. Le strutture di entrambi i minerali sono state raffinate fino a un fattore di accordo  $R_1$ , rispettivamente, di 0.0207 [sulla base di 3418 riflessi unici con  $F_o > 4\sigma(F_o)$ ] e 176 parametri raffinati] e 0.0308 [sulla base di 3074 riflessi unici con  $F_o > 4\sigma(F_o)$ ] e 216 parametri raffinati]. Questi nuovi dati accrescono le conoscenze sulle associazioni secondarie formatesi a seguito dei processi di ossidazione della pirite e consentono una miglior comprensione del sistema di legami a idrogeno presente nella wilcoxite.

**Parole chiave** - epsomite, wilcoxite, solfati, struttura, legami a idrogeno, Fornovolasco, Alpi Apuane

### INTRODUCTION

Magnesium sulfates typically occur in evaporitic deposits, in saline lakes as precipitates, as well as weathering products of coal and ore deposits (Jambor *et al.*, 2000). In particular, the interaction between acidic solutions formed through the weathering of sulfide ores and Mg-rich host rocks (*e.g.*, dolostone) may favour the precipitation of Mg-rich sulfates. Moreover, some Mg sulfates are considered as important phases on other planets and icy moons of the Solar System (*e.g.*, Vaniman *et al.*, 2004; Dyar *et al.*, 2005; Orlando *et al.*, 2005; Chou & Seal II, 2007).

In the framework of a systematic investigation of secondary sulfate assemblages from the pyrite ore deposits from the southern Apuan Alps, Mg-rich sulfate assemblages have been identified in the old tunnels of the Fornovolasco mining complex. Indeed, in addition to the sulfate pile identified and described by Biagioni *et al.* (2011), where volaschioite was first found and where melanterite and römerite were sampled (Mauro *et al.*, 2018a, 2018b), a new sulfate pile was studied, in an area where pyrite ore is hosted at the contact between phyllite and metadolostone. This pile is mainly formed by epsomite and an intermediate member of the series halotrichite/pickeringite, with minor melanterite, gypsum, a copiapite-like mineral, and wilcoxite. In this occurrence, epsomite and wilcoxite occur in crystals suitable for single-crystal X-ray diffraction investigations.

Epsomite,  $Mg(SO_4) \cdot 7H_2O$ , has been known since the beginning of the 19<sup>th</sup> Century (*e.g.*, Jameson, 1805; Delamétherie, 1806). The structure of synthetic  $Mg(SO_4) \cdot 7H_2O$  was first solved by Baur (1964) using film data collected through X-ray diffraction. Ferraris *et al.* (1973) refined the crystal structure using neutron diffraction data on a synthetic sample. Finally, new data were given by Calleri *et al.* (1984) and Fortes *et al.* (2006). Whereas epsomite is well-known from several occurrences world-wide, wilcoxite,  $MgAl(SO_4)_2F \cdot 17H_2O$ , is a rare sulfate species containing F as an additional anion, first reported by Wil-

<sup>(1)</sup> Dipartimento di Scienze della Terra, Università di Pisa, Via Santa Maria 53, I-56126 Pisa

<sup>(2)</sup> Department of Geosciences, Swedish Museum of Natural History, Box 50007, SE-10405 Stockholm, Sweden

Corresponding author: Cristian Biagioni (cristian.biagioni@unipi.it)

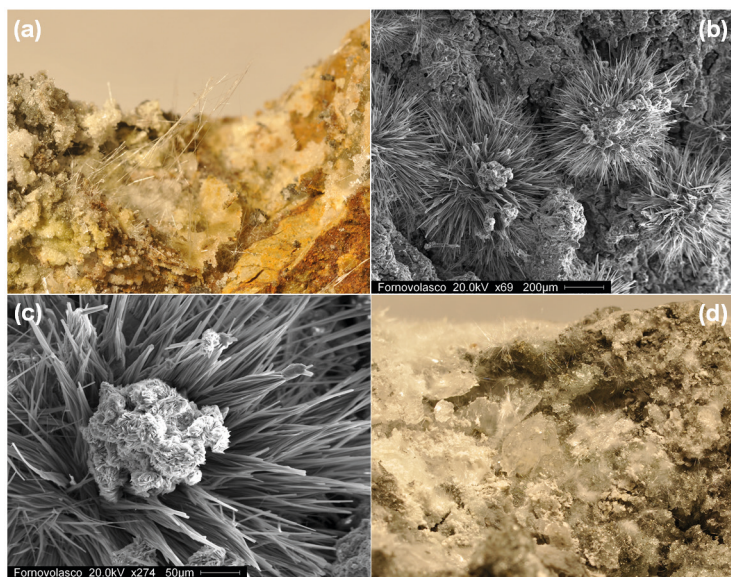


Figure 1. Mg sulfates from the Fornovolasco mining complex. (a) Epsomite, as hairy white acicular crystals, up to 2 cm in length. (b) SEM image of halotrichite/pickeringite, as radial aggregates of acicular crystals. (c) SEM image of an aggregate of micaceous individuals of magnesiocopiapite grown on halotrichite/pickeringite. (d) Colourless crystals of wilcoxite, 4 mm in size, with thin needles of halotrichite/pickeringite.

liams & Cesbron (1983) from the Catron County, New Mexico, USA. The only other Italian occurrence was briefly described by Ciriotti *et al.* (2008) from Punta Chistafort, Gesso Valley, Cuneo, Piedmont. The crystal structure of wilcoxite was recently solved by Peterson & Joy (2013) using a sample from Rico, Colorado, USA.

The aim of this paper is manifold. It describes the phases identified in the Mg-rich sulfate assemblages from the Fornovolasco mining complex, reporting and briefly discussing their Raman and infrared spectra. In addition, the paper reports the results of the crystal structure refinements performed on epsomite and wilcoxite. To the best of our knowledge, no crystal structure data obtained on natural samples of epsomite have been reported in literature so far, whereas the new data collected on wilcoxite improves the knowledge on this rare sulfate and its hydrogen bond system.

## EXPERIMENTAL

The studied specimens (Fig. 1) were collected in the old tunnels of the pyrite – iron oxide mine of Fornovolasco (Fabbriche di Vergemoli, Apuan Alps, Tuscany, Italy). Their identification was based on X-ray powder diffraction patterns collected using a 114.6 mm Gandolfi camera and Ni-filtered  $\text{CuK}\alpha$  radiation.

Epsomite (Fig. 1a) shows different habits: i) anhedral equant colourless grains, ii) prismatic colourless crystals, up to 1 mm in length, and iii) thin acicular individuals, up to 3 cm long. The crystal used for the single-crystal X-ray diffraction study is represented by type ii). Halotrichite/pickeringite (Fig. 1b) occurs as hairy whitish needles or as rounded aggregates of acicular crystals. Magnesiocopiapite (Fig. 1c) forms flow-

er-like aggregates of mica-like yellow crystals, associated with halotrichite/pickeringite. Finally, wilcoxite (Fig. 1d) occurs as colourless to whitish crystals, up to 5 mm in size, having a distinct triclinic symmetry, in some cases showing rounded edges.

## Chemical data

Accurate electron microprobe chemical analysis of hydrated sulfates represents a difficult task, due to their instability under the electron beam and the high vacuum, resulting in their rapid dehydration. In addition, fluid inclusions entrapped in sulfates can rapidly burst, destroying the carbon coating and the polished surface of the studied grains. This is particular critical for wilcoxite. Indeed, as described by Williams & Cesbron (1983), this mineral dissolves in its crystallization water upon heating. For these reasons, chemical analyses were performed using a Philips XL30 scanning electron microscope equipped with an EDAX DX4 spectrometer operating in energy-dispersive mode (EDS). Taking into account the difficulties in obtaining good chemical analyses, the chemistry of the studied samples will be discussed only qualitatively. Epsomite shows Mg, S, and minor Fe as the only elements with  $Z > 8$ . The iron-to-magnesium substitution is low but not negligible, as confirmed by single-crystal structure refinement (see below). Members of the halotrichite/pickeringite series show variable Mg/Fe ratios, with Al and S as additional detected elements. The compositions are close to the boundary between halotrichite (Fe-dominant) and pickeringite (Mg-dominant). The member of the copiapite group occurring in the studied assemblage was attributed to magnesiocopiapite. Indeed, the recalculation of the chemical data

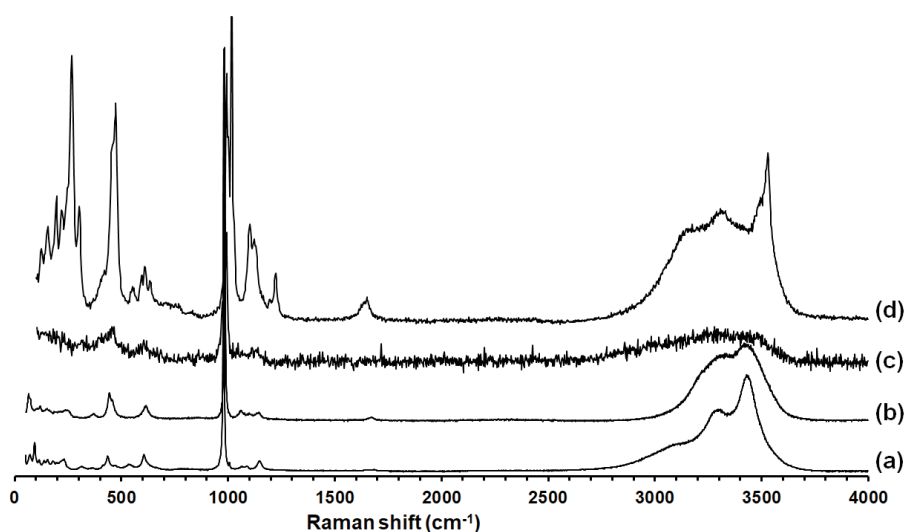


Figure 2. Raman spectra of wilcoxite (a), epsomite (b), halotrichite/pickeringite (c), and magnesiocopiapite (d).

on the basis of 25 O atoms per formula unit, assuming the occurrence of 2 OH and 20 H<sub>2</sub>O groups, is Mg<sub>1.29</sub>(Fe<sub>3.84</sub>Al<sub>0.11</sub>)<sub>Σ3.95</sub>(S<sub>5.93</sub>O<sub>24</sub>)(OH)<sub>2</sub>·20H<sub>2</sub>O, in reasonable agreement with the end-member formula MgFe<sub>4</sub>(SO<sub>4</sub>)<sub>6</sub>(OH)<sub>2</sub>·20H<sub>2</sub>O. Finally, Mg, Al, S, F, and minor Fe were the elements detected in wilcoxite. Also in this case, minor replacement of Mg by Fe is confirmed by the crystal structure refinement (see below).

#### Micro-Raman and FTIR spectroscopies

Unpolarized micro-Raman spectra were collected on unpolished samples of epsomite, halotrichite/pickeringite, magnesiocopiapite, and wilcoxite in nearly back-scattered geometry with a Jobin-Yvon Horiba XploRA Plus apparatus, equipped with a motorized *x-y* stage and an Olympus BX41 microscope with a 10× objective lens. The Raman spectra were excited using a 532 nm line of a solid-state laser attenuated to 10% in order to minimize sample damage. The minimum lateral and depth resolution was set to a few μm. The system was calibrated using the 520.6 cm<sup>-1</sup> Raman band of silicon before each experimental session. Spectra were collected from 100 to 4000 cm<sup>-1</sup> through multiple acquisitions with single counting times of 60 s. Back-scattered radiation was analyzed with a 1200 gr/mm grating monochromator.

Raman spectra of the studied phases are shown in Fig. 2. The position of the observed bands and their interpretation are given in Tab. 1. The main feature observed in the Raman spectra of the minerals occurring in the studied sulfate assemblage is represented by the vibrational modes of SO<sub>4</sub> groups, in the spectral range between 400 to 1300 cm<sup>-1</sup>. The strongest bands, occurring in the range between

800 to 1005 cm<sup>-1</sup>, are related to the symmetrical SO<sub>4</sub> stretching vibration mode  $\nu_1$ . The bands in the range between 1010 to 1230 cm<sup>-1</sup> can be assigned to the antisymmetrical SO<sub>4</sub> stretching mode  $\nu_3$ . The bending modes of the SO<sub>4</sub> groups are represented by bands in the region between 400 and 480 cm<sup>-1</sup> ( $\nu_2$  mode) and 580 to 640 cm<sup>-1</sup> ( $\nu_4$  mode), respectively. The occurrence of multiple bands for the SO<sub>4</sub> groups for halotrichite/pickeringite and magnesiocopiapite is in keeping with the presence of structurally different SO<sub>4</sub> units, in agreement with previous authors (*e.g.*, Locke *et al.*, 2007; Kong *et al.*, 2011) and confirmed by the crystal structure features of these minerals (*e.g.*, Quartieri *et al.*, 2000; Majzlan & Kiefer, 2006). Raman bands at wavenumbers lower than 400 cm<sup>-1</sup> can be attributed to *Me*-O vibrational modes, where *Me* = Fe, Al, Mg. The hydrated nature of the studied phases is confirmed by the occurrence of relatively strong and broad bands between 3000 and 4000 cm<sup>-1</sup>. In the Raman spectrum of magnesiocopiapite, the band at 3528 cm<sup>-1</sup> can be related to the stretching mode of the O-H bond in hydroxyl groups, in agreement with Kong *et al.* (2011). Finally, bending modes of H<sub>2</sub>O groups were observed in the Raman spectra of epsomite and magnesiocopiapite at 1670 and 1644 cm<sup>-1</sup>, respectively.

Unpolarized FTIR absorption spectra were measured using a Bruker Vertex 70 spectrometer equipped with a Hyperion 2000 microscope, a Global source, a KBr beam-splitter, and a MCT detector. Data were acquired during 128 scans in the range 4000-600 cm<sup>-1</sup> with a resolution of 2 cm<sup>-1</sup>. Crystal thickness varied between 50 and 150 μm. Cracks and inclusions in the crystals were avoided by applying small aperture (30 to 100 μm) for masking during analyses. The FTIR absorption spectra allowed the description, for all the studied samples,

Table 1. Raman bands ( $\text{cm}^{-1}$ ) and band assignments of the studied sulfates. In addition, bending modes observed through FTIR are given within parentheses.

Wilcoxite	Epsomite	Halotrichite/pickeringite	Magnesiocopiapite	Assignments
75	117	233	125	
95	294		155	
154	372		183	
232			195	
			220	$Me-O$ and lattice modes
			243	
			268	
			303	
			390	
436	444	424	420	
		468	455	$\nu_2(\text{SO}_4)$
			474	
606	614	621	594	
			610	$\nu_4(\text{SO}_4)$
			635	
979	984	975	992	
		996	1004	$\nu_1(\text{SO}_4)$
1006	1061	1071	1025	
1146	1099	1114	1101	
	1145	1145	1124	$\nu_3(\text{SO}_4)$
			1222	
(1643)	1670, (1675)	(1649)	1644, (1635, 1689)	
2981	3197	3082	3164	
3084	3419	3279	3315	$\nu(\text{H}_2\text{O})$
3264		3449	3500	
			3528	

of the  $\nu_2$  bending mode of the  $\text{H}_2\text{O}$  groups. This spectral feature was not observed or was very weak in the collected Raman spectra. The  $\text{H}_2\text{O}$  bending modes of epsomite, halotrichite/pickeringite, magnesiocopiapite, and wilcoxite were observed at 1675, 1649, 1635, and 1643  $\text{cm}^{-1}$ , respectively. These band positions can be compared with those reported in literature (in  $\text{cm}^{-1}$ ): 1670 (epsomite – Wang *et al.*, 2006), 1650 (halotrichite/pickeringite – Locke *et al.*, 2007), 1637 (copiapite group minerals – Majzlan & Michallik, 2007), and 1640 (wilcoxite – Peterson & Joy, 2013). In all the collected FTIR spectra, the  $\text{H}_2\text{O}$  bending mode vibration shows more or less pronounced shoulder features (*e.g.*, at 1689  $\text{cm}^{-1}$  in the spectrum of magnesiocopiapite, where this should may be considered as a distinct band), indicating the occurrence of slightly different  $\text{H}_2\text{O}$  environments

in the crystal structure of the studied minerals. Tab. 1 gives the position of the observed bands.

#### *X-ray crystallography*

Owing to the lack of suitable crystals of halotrichite/pickeringite and magnesiocopiapite, single-crystal X-ray diffraction studies were carried out for epsomite and wilcoxite only. Intensity data were collected using a Bruker Smart Breeze diffractometer operating at 50 kV and 30 mA and equipped with an air-cooled CCD detector. Graphite-monochromatized MoK $\alpha$  radiation was used. The detector-to-crystal working distance was set to 50 mm. Intensity data were integrated and corrected for Lorentz, polarization, background effects, and absorption using the

Table 2. Crystal data and summary of parameters describing data collections and refinements for epsomite and wilcoxite.

Crystal data		
	Epsomite	Wilcoxite
Crystal size (mm)	0.22 × 0.12 × 0.12	0.18 × 0.15 × 0.13
Cell setting, space group	$P2_12_12_1$	$P\bar{1}$
$a$ (Å)	11.8664(3)	6.6749(4)
$b$ (Å)	12.0150(3)	6.7730(4)
$c$ (Å)	6.8598(2)	14.9076(9)
$\alpha$ (°)	90	79.604(3)
$\beta$ (°)	90	80.163(3)
$\gamma$ (°)	90	62.475(3)
$V$ (Å <sup>3</sup> )	978.03(4)	584.90(6)
$Z$	4	1
Data collection and refinement		
Radiation, wavelength (Å)	MoK $\alpha$ , $\lambda = 0.71073$	MoK $\alpha$ , $\lambda = 0.71073$
Temperature (K)	293	293
Maximum observed $2\theta$ (°)	64.89	63.49
Measured reflections	29806	11790
Unique reflections	3520	3606
Reflections $F_o > 4\sigma(F_o)$	3418	3074
$R_{\text{int}}$ after absorption correction	0.0232	0.0186
$R\sigma$	0.0170	0.0201
Range of $h, k, l$	-17 ≤ $h$ ≤ 17 -18 ≤ $k$ ≤ 18 -10 ≤ $l$ ≤ 10	-8 ≤ $h$ ≤ 9 -10 ≤ $k$ ≤ 9 -21 ≤ $l$ ≤ 18
$R_1$ [ $F_o > 4\sigma(F_o)$ ]	0.0207	0.0308
$R_1$ (all data)	0.0215	0.0388
$wR_2$ (on $F_o^2$ )	0.0537	0.0848
Goodness of fit	1.095	0.997
Number of least-squares parameters	176	216
Maximum and minum residual peak ( $e/\text{Å}^3$ )	0.38 (at 0.71 Å from S) -0.18 (at 0.51 Å from S)	0.42 [at 0.68 Å from O(3)] -0.25 (at 0.43 Å from S)

package of software *Apex 2* (Bruker AXS Inc., 2004). Epsomite is orthorhombic, space group  $P2_12_12_1$ , with unit-cell parameters  $a = 11.8664(3)$ ,  $b = 12.0150(3)$ ,  $c = 6.8598(2)$  Å,  $V = 978.03(4)$  Å<sup>3</sup>. Wilcoxite is triclinic, space group  $P\bar{1}$ , with unit-cell parameters  $a = 6.6749(4)$ ,  $b = 6.7730(4)$ ,  $c = 14.9076(9)$  Å,  $\alpha = 79.604(3)$ ,  $\beta = 80.163(3)$ ,  $\gamma = 62.475(3)^\circ$ ,  $V = 584.90(6)$  Å<sup>3</sup>. The crystal structures of both minerals were refined using *Shelxl-2018* (Sheldrick, 2015), starting from the atomic coordinates given by Fortes *et al.* (2006) and by Peterson & Joy (2013) for epsomite and wilcoxite, respectively. Taking into account the results of chemical analyses, the following neutral scattering curves, taken from the International Tables for Crystallography (Wilson, 1992), were used: Mg *vs* Fe at the Mg site, S at the S site, O at the O sites, and H at the H sites.

In addition, for wilcoxite only, the scattering curves of Al and F were used at the Al and F sites, respectively. A soft restraint was applied on the O–H distances, in order to avoid too short values. After several cycles of anisotropic refinement (with the exception of H atoms, which were refined isotropically), the crystal structure refinements of epsomite and wilcoxite converged to  $R_1 = 0.0207$  [for 3418 unique reflections with  $F_o > 4\sigma(F_o)$  and 176 refined parameters] and 0.0308 [for 3074 unique reflections with  $F_o > 4\sigma(F_o)$  and 216 refined parameters] for epsomite and wilcoxite, respectively. Details of data collections and crystal structure refinements are given in Tab. 2. Fractional atomic coordinates, site occupancies, and displacement parameters are reported in Tabs 3 and 4, whereas Tab. 5 shows selected bond distances.

Table 3. Sites, site occupancy factors (s.o.f.), fractional atomic coordinates, and isotropic (\*) or equivalent isotropic displacement parameters ( $\text{\AA}^2$ ) for epsomite.

Site	s.o.f.	x/a	y/b	z/c	$U_{\text{eq/iso}}$
Mg	$\text{Mg}_{0.83(1)}\text{Fe}_{0.17(1)}$	0.42307(3)	0.10666(3)	0.03998(5)	0.01895(12)
S	$\text{S}_{1.00}$	0.72671(2)	0.18390(2)	0.49056(4)	0.01919(7)
O(1)	$\text{O}_{1.00}$	0.68563(13)	0.07497(10)	0.42743(19)	0.0416(3)
O(2)	$\text{O}_{1.00}$	0.85051(8)	0.18723(11)	0.48306(16)	0.0329(2)
O(3)	$\text{O}_{1.00}$	0.68859(10)	0.20572(11)	0.69079(16)	0.0363(3)
O(4)	$\text{O}_{1.00}$	0.68038(9)	0.27211(9)	0.36226(17)	0.0306(2)
Ow(1)	$\text{O}_{1.00}$	0.26452(8)	0.17420(10)	0.00317(15)	0.0314(2)
Ow(2)	$\text{O}_{1.00}$	0.47177(8)	0.24888(8)	0.19781(16)	0.02482(18)
Ow(3)	$\text{O}_{1.00}$	0.46905(9)	0.17613(10)	0.77872(16)	0.0312(2)
Ow(4)	$\text{O}_{1.00}$	0.58379(10)	0.04676(11)	0.07662(18)	0.0370(3)
Ow(5)	$\text{O}_{1.00}$	0.37590(10)	0.96104(9)	0.88973(17)	0.0292(2)
Ow(6)	$\text{O}_{1.00}$	0.36262(10)	0.03404(11)	0.29158(18)	0.0345(2)
Ow(7)	$\text{O}_{1.00}$	0.49139(11)	0.43836(10)	0.9384(2)	0.0367(2)
H(11)	$\text{H}_{1.00}$	0.238(3)	0.203(3)	0.883(4)	0.067(9)*
H(12)	$\text{H}_{1.00}$	0.238(3)	0.218(3)	0.094(5)	0.080(11)*
H(21)	$\text{H}_{1.00}$	0.537(2)	0.249(2)	0.246(4)	0.045(7)*
H(22)	$\text{H}_{1.00}$	0.431(2)	0.2637(18)	0.295(3)	0.034(5)*
H(31)	$\text{H}_{1.00}$	0.5359(19)	0.183(2)	0.750(4)	0.041(6)*
H(32)	$\text{H}_{1.00}$	0.429(2)	0.219(2)	0.695(4)	0.051(7)*
H(41)	$\text{H}_{1.00}$	0.612(3)	0.981(3)	0.032(6)	0.080(10)*
H(42)	$\text{H}_{1.00}$	0.625(2)	0.059(2)	0.185(4)	0.052(7)*
H(51)	$\text{H}_{1.00}$	0.416(2)	0.947(2)	0.790(4)	0.044(6)*
H(52)	$\text{H}_{1.00}$	0.364(2)	0.898(2)	0.948(4)	0.043(6)*
H(61)	$\text{H}_{1.00}$	0.397(2)	0.007(2)	0.383(4)	0.051(7)*
H(62)	$\text{H}_{1.00}$	0.294(2)	0.025(2)	0.319(4)	0.044(6)*
H(71)	$\text{H}_{1.00}$	0.476(2)	0.380(2)	0.989(4)	0.041(6)*
H(72)	$\text{H}_{1.00}$	0.429(2)	0.475(3)	0.955(5)	0.066(9)*

## DESCRIPTION OF THE CRYSTAL STRUCTURE

*General features, cation coordination, and hydrogen bonding in epsomite*

The general features of the crystal structure of epsomite agree with those reported by previous authors (Baur, 1964; Ferraris *et al.*, 1973; Calleri *et al.*, 1984; Fortes *et al.*, 2006). It is formed by isolated  $\text{Mg}(\text{H}_2\text{O})_6$  octahedra connected, through H-bonding, to isolated  $\text{SO}_4$  groups. An interstitial isolated  $\text{H}_2\text{O}$  group completes the structure (Fig. 3).

Magnesium is hosted at the Mg site and it is octahedrally coordinated by  $\text{H}_2\text{O}$  groups. The refinement of the site occupation factor (s.o.f.) points to a mixed (Mg,Fe) occupancy,  $\text{Mg}_{0.84}\text{Fe}_{0.16}$ , agreeing with the chemical data which show a minor replacement of Mg by Fe. Bond distances range between 2.05 and 2.11 Å,

with an average distance of 2.074 Å. This value can be compared with those observed by previous authors at room temperature, *i.e.*, 2.065 Å (Baur, 1964), 2.072 Å (Ferraris *et al.*, 1973), and 2.070 Å (Calleri *et al.*, 1984). Using the ionic radii given by Shannon (1976) for  $\text{VI}\text{Mg}^{2+}$  (0.72 Å),  $\text{VI}\text{Fe}^{2+}$  (0.78 Å), and  $\text{III}\text{O}^{2-}$  (1.36 Å), the ideal average distance of 2.09 Å for the Mg site can be calculated, slightly larger than the observed value. The bond-valence sum (BVS), reported in Tab. 6, is 2.19 valence unit (v.u.), slightly higher than the expected value.

The isolated  $\text{SO}_4$  group has average  $\langle\text{S}-\text{O}\rangle$  of 1.471 Å, in good agreement with the average  $\langle\text{S}-\text{O}\rangle$  distance in sulfates reported by Hawthorne *et al.* (2000), *i.e.*, 1.473 Å. The BVS is 6.04 v.u.

The Mg-centered octahedra and the S-centered tetrahedra are connected through H-bonds. The examina-

Table 4. Sites, site occupancy factors (s.o.f.), fractional atomic coordinates, and isotropic (\*) or equivalent isotropic displacement parameters ( $\text{\AA}^2$ ) for wilcoxite.

Site	s.o.f.	$x/a$	$y/b$	$z/c$	$U_{\text{eq/iso}}$
Mg	$\text{Mg}_{0.98(1)}\text{Fe}_{0.02(1)}$	0	0	0	0.0246(2)
Al	$\text{Al}_{1.00}$	$\frac{1}{2}$	0	$\frac{1}{2}$	0.01990(11)
S	$\text{S}_{1.00}$	0.58846(5)	0.55014(4)	0.24375(2)	0.02276(9)
O(1)	$\text{O}_{1.00}$	0.4854(2)	0.39492(18)	0.26131(7)	0.0394(2)
O(2)	$\text{O}_{1.00}$	0.61188(17)	0.62214(16)	0.14529(6)	0.0342(2)
O(3)	$\text{O}_{1.00}$	0.44607(16)	0.74609(17)	0.29381(8)	0.0391(2)
O(4)	$\text{O}_{1.00}$	0.81637(16)	0.43509(17)	0.27740(7)	0.0348(2)
F/Ow(1)	$\text{F}_{0.50}\text{O}_{0.50}$	0.24845(14)	0.98315(14)	0.48149(6)	0.03029(18)
Ow(5)	$\text{O}_{1.00}$	0.61815(17)	0.70355(15)	0.56124(7)	0.0319(2)
Ow(6)	$\text{O}_{1.00}$	0.64275(16)	0.88384(15)	0.38889(6)	0.02773(19)
Ow(7)	$\text{O}_{1.00}$	0.24287(19)	0.99693(18)	0.06922(8)	0.0382(2)
Ow(8)	$\text{O}_{1.00}$	0.8159(2)	0.33909(17)	0.00567(8)	0.0412(3)
Ow(9)	$\text{O}_{1.00}$	0.1673(2)	0.06829(19)	0.87675(7)	0.0405(2)
Ow(10)	$\text{O}_{1.00}$	0.20815(19)	0.35619(18)	0.14914(8)	0.0370(2)
Ow(11)	$\text{O}_{1.00}$	0.14846(17)	0.64355(15)	0.53701(7)	0.0320(2)
Ow(12)	$\text{O}_{1.00}$	0.97421(18)	0.95812(18)	0.28869(7)	0.0350(2)
H(11)	$\text{H}_{0.50}$	0.120(6)	0.108(6)	0.474(3)	0.063(12)*
H(12)	$\text{H}_{0.50}$	0.228(7)	0.861(5)	0.495(3)	0.054(11)*
H(51)	$\text{H}_{1.00}$	0.697(4)	0.589(3)	0.5336(14)	0.059(6)*
H(52)	$\text{H}_{1.00}$	0.579(3)	0.673(3)	0.6170(13)	0.053(6)*
H(61)	$\text{H}_{1.00}$	0.578(4)	0.843(3)	0.3553(14)	0.058(6)*
H(62)	$\text{H}_{1.00}$	0.755(3)	0.906(3)	0.3588(14)	0.055(6)*
H(71)	$\text{H}_{1.00}$	0.357(3)	0.884(3)	0.0885(15)	0.061(6)*
H(72)	$\text{H}_{1.00}$	0.240(4)	0.108(4)	0.0918(17)	0.078(7)*
H(81)	$\text{H}_{1.00}$	0.749(4)	0.408(4)	0.0488(16)	0.060(6)*
H(82)	$\text{H}_{1.00}$	0.813(4)	0.429(4)	0.963(16)	0.061(6)*
H(91)	$\text{H}_{1.00}$	0.234(4)	0.158(4)	0.8679(18)	0.083(8)*
H(92)	$\text{H}_{1.00}$	0.129(4)	0.070(4)	0.8254(14)	0.059(6)*
H(101)	$\text{H}_{1.00}$	0.080(4)	0.399(4)	0.1868(16)	0.069(7)*
H(102)	$\text{H}_{1.00}$	0.309(3)	0.347(3)	0.1806(14)	0.056(6)*
H(111)	$\text{H}_{0.50}$	0.217(8)	0.735(7)	0.518(3)	0.078(10)*
H(112)	$\text{H}_{0.50}$	0.995(5)	0.722(8)	0.543(3)	0.078(10)*
H(113)	$\text{H}_{1.00}$	0.174(4)	0.590(3)	0.5949(13)	0.055(6)*
H(121)	$\text{H}_{1.00}$	0.112(4)	0.902(4)	0.2934(16)	0.064(6)*
H(122)	$\text{H}_{1.00}$	0.941(3)	0.091(4)	0.2846(14)	0.052(6)*

tion of the BVS values of the atoms hosted at the eleven independent anion sites indicate that all the oxygen atoms are underbonded. Indeed, the oxygen atoms bonded to S have BVS ranging between 1.46 and 1.55 v.u., whereas the oxygen atoms bonded to Mg show BVS between 0.33 and 0.39 v.u. Finally, Ow(7) is not bonded to any cation.

The location of H atoms allows to confirm the H-bonding previously reported by Baur (1964) and Ferraris *et al.* (1973). Tab. 7 gives the geometrical features of the H-bonds observed in epsomite. Oxygen atoms belonging to  $\text{SO}_4$  groups are acceptor of two or three H-bonds from  $\text{H}_2\text{O}$  groups, whereas the oxygen atoms coordinating Mg usually act as donor of

Table 5. Selected bond distances (Å) for epsomite and wilcoxite.

Epsomite			Wilcoxite		
Mg	– Ow(3)	2.0509(11)	Mg	– Ow(8)	2.0538(10) ×2
	– Ow(4)	2.0539(11)		– Ow(7)	2.0557(10) ×2
	– Ow(6)	2.0627(12)		– Ow(9)	2.0751(10) ×2
	– Ow(1)	2.0644(10)		average	2.062
	– Ow(2)	2.1038(10)			
	– Ow(5)	2.1064(11)	Al	– F/Ow(1)	1.8043(8) ×2
	average	2.074		– Ow(6)	1.8731(9) ×2
				– Ow(5)	1.8994(9) ×2
				average	1.859
S	– O(1)	1.4623(11)	S	– O(2)	1.4665(10)
	– O(3)	1.4696(11)		– O(1)	1.4681(10)
	– O(2)	1.4705(10)		– O(3)	1.4734(10)
	– O(4)	1.4833(10)		– O(4)	1.4823(10)
	average	1.471		average	1.473

H-bonds. The only exception is represented by the oxygen atoms at the Ow(2) and Ow(5) sites that are also acceptor of H-bonds from Ow(7) and Ow(6), respectively. The oxygen atom at the Ow(7) site acts both as acceptor and donor of H-bonds. Taking into account the O...O distances and applying the relationship of Ferraris & Ivaldi (1988) between bond distance and bond strength, the corrected values of BVS at the oxygen atoms of the SO<sub>4</sub> group range between 1.95 and 2.03 v.u., whereas H<sub>2</sub>O groups have BVS in the range -0.05-0.18 v.u.

Hydrogen-bonds are fundamental in connecting the isolated polyhedra in the crystal structure of epsomite. Taking into account the shortest (*i.e.*, the strongest) H...O bonds (H...O < 1.95 Å), undulating layers running along **a** can be highlighted (Fig. 3), showing the alternation of SO<sub>4</sub> groups and Mg(H<sub>2</sub>O)<sub>6</sub> octahedra. The seventh H<sub>2</sub>O group is located between the undulating layers. In order to stress the different role played by H<sub>2</sub>O groups, the ideal end-member formula of epsomite should be written as Mg(SO<sub>4</sub>)(H<sub>2</sub>O)<sub>6</sub>·H<sub>2</sub>O.

#### General features, cation coordination, and hydrogen bonding in wilcoxite

The crystal structure of wilcoxite (Fig.4a) is formed by rows of isolated Mg(H<sub>2</sub>O)<sub>6</sub> octahedra, alternating, along **c**, with rows of isolated SO<sub>4</sub> groups and rows of isolated Al(H<sub>2</sub>O,F)<sub>6</sub> octahedra, in agreement with the structure solution first proposed by Peterson & Joy (2013). Three H<sub>2</sub>O groups are not directly bonded to cations.

Magnesium is hosted at Mg site and it is octahedrally coordinated by H<sub>2</sub>O groups. The refinement of the s.o.f. indicates the occurrence of a negligible content of heavier atoms. Bond distances range between 2.05 and 2.08 Å, with an average distance of 2.062 Å, shorter than the ideal value of 2.08 Å calculated using the ionic radii of Shannon (1976). This results in a slight overbonding of Mg, 2.21 v.u. Peterson & Joy (2013) found a similar <Mg–O> distance of 2.065 Å, with values ranging from 2.06 and 2.08 Å.

Aluminum is octahedrally coordinated by five H<sub>2</sub>O groups and one F anion. Fluorine and an oxygen atom, attributed to an H<sub>2</sub>O group, statistically occupy two opposite vertices of the Al-centered octahedron. Peterson & Joy (2013) assigned F at the anion site forming the shorter Al–O distance, *i.e.*, 1.805 Å. During the present refinement, the occurrence of a residual maximum around the (F,O) site was interpreted as due to the actual splitting of this site, showing a shorter Al–F (≈ 1.75 Å) and a longer Al–(H<sub>2</sub>O) (≈ 1.93 Å) distance. However, such a model did not allow to find the residual maxima attributed to the H atoms of the H<sub>2</sub>O groups. Consequently, an unsplit model was preferred, since it allowed a better description of the H-bond system occurring in wilcoxite. The Al-centered octahedron has an average bond distance of 1.86 Å, and a BVS of 3.22 v.u.

The SO<sub>4</sub> group has average <S–O> of 1.473 Å, in perfect agreement with the average <S–O> distance in sulfates reported by Hawthorne *et al.* (2000), and matching the value reported by Peterson & Joy (2013), 1.476 Å. Its BVS is 6.02 v.u.

As in epsomite, all the oxygen atoms occurring in the crystal structure of wilcoxite are underbonded (Tab. 6), stressing the role played by the H-bonds. Their geometrical features are reported in Tab. 8. The H<sub>2</sub>O groups coordinating Mg and Al, namely Ow(5)-Ow(9), are donor of H-bonds to the oxygen atoms belonging to the SO<sub>4</sub> group or to the non-bonded H<sub>2</sub>O groups. The F/Ow site coordinating Al acts as donor of H-bonds to Ow(11) when it is occupied by H<sub>2</sub>O. On the contrary, it is acceptor of H-bonds when it is occupied by F. The role of F as acceptor of H-bonds has been observed in other rare sulfates (*e.g.*, khademite, Al(SO<sub>4</sub>)F·5H<sub>2</sub>O – Bacht *et al.*, 1981). The three H<sub>2</sub>O groups not bonded to cations are acceptor of H-bonds from H<sub>2</sub>O groups coordinating Mg and Al, and act as donor to the oxygen atoms of the SO<sub>4</sub> groups or to the F atom.

Fig. 4b shows the H-bonds involving Ow(11), Ow(1), and F. Ow(11) is donor of H-bond to O(4) (0.20 v.u.) and is acceptor from Ow(5) (0.24 v.u.) and Ow(1). Two slightly different Ow(1)–H...Ow(11) distances occur, corresponding to bond-strengths, calculated taking into account the O...O distances and the rela-

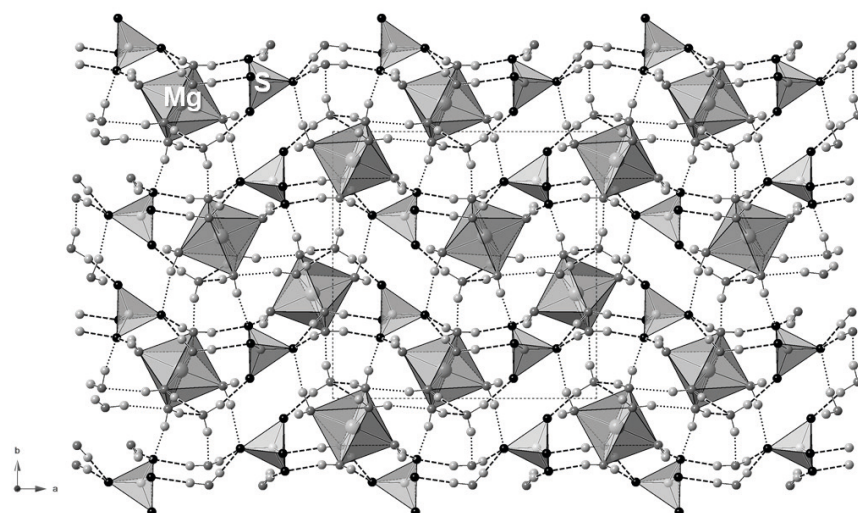


Figure 3. Projection along *c* of the crystal structure of epsomite. Circles represent O atoms (black), H<sub>2</sub>O groups (medium-grey), or H atoms (light grey). Dashed and dotted lines represent H...O distances shorter and longer than 1.95 Å, respectively.

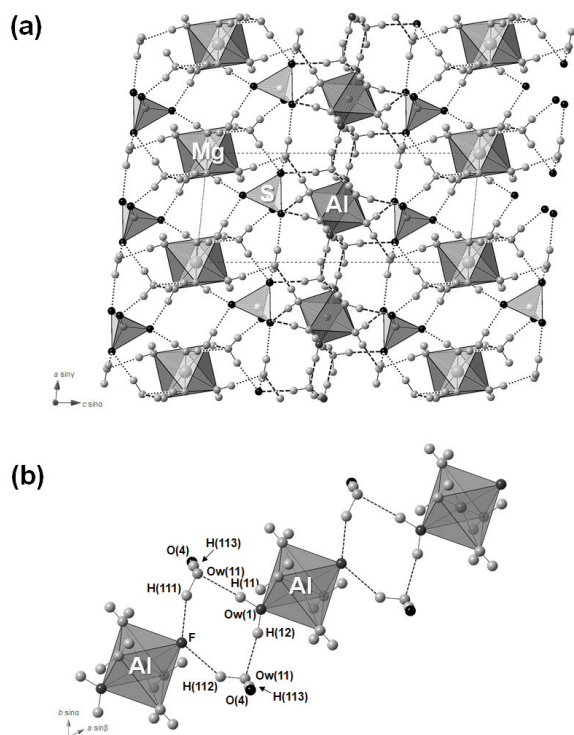


Figure 4. The crystal structure of wilcoxite as seen down *b* (a) and the hydrogen bonding system involving the F/Ow(1) and Ow(11) sites as seen down *c* (b). Same symbols as in Fig. 3.

tionship of Ferraris & Ivaldi (1988), of 0.23 and 0.26 v.u. Consequently, the total BVS at Ow(11) is 0.27 or 0.30 v.u., before taking into account the Ow(11)–H...F bond. Indeed, Ow(11) is donor of H-bond to F with two slightly different configurations involving H(111) and H(112). Geometrical features agree with those of H-bonds; although the Ow(11)–H(112) ···F is

relatively small, it is still in the angular range reported by Brown (1976).

The calculation of the bond strength of the O...F bond is not straightforward. Brown & Altermatt (1985) discussed the evaluation of the bond strength of O...X hydrogen bonds, where X is a variety of anions (*e.g.*, F, N, Cl, Br, S, I). Since X-ray diffraction allows the location of the centroid of the electron density rather than the actual H nucleus position, the H atom appears to be closer to the donor than it actually is. This phenomenon has to be combined with the uncertainties in the accurate determination of H atomic coordinates. Consequently, Brown & Altermatt (1985) suggest to constrain the H atom to a position about 1.0 Å from the donor. In this case, the H(111)···F and H(112)···F distances are 1.68 and 1.87 Å, respectively. Using the bond-valence parameters for the pair (H,F) reported by Brese & O'Keefe (1991), the bond strength of 0.13 and 0.08 v.u. can be obtained for these hydrogen bonds. In this way, F atom has a total BVS of 0.78 v.u., and Ow(11) a BVS ranging between 0.17 and 0.19 v.u. An alternative and more qualitative approach assumes that the theoretical BVS of Ow(11) should approach 0 v.u. In this way, the BVS excess should be attributed to F, that in this way would achieve a total BVS of 1.14 v.u.

Wilcoxite is thus an interesting example of a fluo-sulfate mineral, characterized by a complex H-bond system. With respect to the previous structural determination reported by Peterson & Joy (2013), the present refinement clarifies the H-bonding system involving the F/Ow(1) and Ow(11) sites. Finally, taking into account the different bonding environments shown by H<sub>2</sub>O groups, the end-member formula of wilcoxite should be written as MgAl(SO<sub>4</sub>)<sub>2</sub>F(H<sub>2</sub>O)<sub>11</sub>·6H<sub>2</sub>O.

Table 6. Weighted bond-valence sums (BVS) for epsomite and wilcoxite.

Epsomite					Wilcoxite					
Site	Mg	S	$\Sigma\nu_a$	$\Sigma\nu_a(\text{corr})$	Site	Mg	Al	S	$\Sigma\nu_a$	$\Sigma\nu_a(\text{corr})$
O(1)		1.55	1.55	1.95	O(1)			1.52	1.52	1.95
O(2)		1.51	1.51	2.03	O(2)			1.53	1.53	2.02
O(3)		1.52	1.52	1.98	O(3)			1.50	1.50	1.96
O(4)		1.46	1.46	2.01	O(4)			1.47	1.47	2.00
Ow(1)	0.37		0.37	-0.05	F/Ow(1)		0.57 <sup>1×2</sup>		0.57	0.78 <sup>1</sup> 0.08 <sup>2</sup>
Ow(2)	0.34		0.34	0.07	Ow(5)		0.50 <sup>1×2</sup>		0.50	0.01
Ow(3)	0.39		0.39	-0.02	Ow(6)		0.54 <sup>1×2</sup>		0.54	0.00
Ow(4)	0.38		0.38	0.03	Ow(7)	0.38 <sup>1×2</sup>			0.38	0.02
Ow(5)	0.33		0.33	0.18	Ow(8)	0.38 <sup>1×2</sup>			0.38	0.01
Ow(6)	0.38		0.38	0.04	Ow(9)	0.36 <sup>1×2</sup>			0.36	0.06
Ow(7)			0.00	0.06	Ow(10)				0.00	0.02
					Ow(11)				0.00	0.17/0.19
					Ow(12)				0.00	0.09
$\Sigma\nu_c$	2.19	6.04			$\Sigma\nu_c$	2.24	3.22	6.02		

Note: right superscripts indicate the number of equivalent bonds involving cations. For sites with mixed occupancy, BVS have been weighted according to the proposed site population.  $\Sigma\nu_c$  = BVS over cations;  $\Sigma\nu_a$  = BVS over anions.  $\Sigma\nu_a(\text{corr})$  = BVS corrected taking into account H-bonds. Bond parameters after Brese & O'Keeffe (1991) were used. At the F/Ow(1) site, superscript 1 indicates BVS when F is acceptor of H-bonds; superscript 2 indicates BVS when Ow(1) is donor of H-bonds. At Ow(11), the two slightly different values indicate BVS assuming two different configurations shown in Fig. 4b.

Table 7. Hydrogen-bond lengths (Å) and angles (°) for epsomite.

Donor (D)	D–H	Acceptor (A)	H...A	D–H...A angle	D...A
Ow(1)–H(11)	0.95(3)	O(4)	1.84(3)	167(3)	2.7743(15)
Ow(1)–H(12)	0.88(3)	O(3)	1.83(3)	172(4)	2.7020(15)
Ow(2)–H(21)	0.84(2)	O(4)	1.90(2)	171(3)	2.7346(14)
Ow(2)–H(22)	0.84(2)	O(2)	1.89(2)	173(2)	2.7299(15)
Ow(3)–H(31)	0.83(2)	O(3)	1.87(2)	177(2)	2.6976(15)
Ow(3)–H(32)	0.90(2)	O(2)	1.91(3)	178(3)	2.8105(16)
Ow(4)–H(41)	0.91(3)	O(2)	2.10(3)	165(3)	2.9872(17)
Ow(4)–H(42)	0.90(3)	O(1)	1.82(3)	169(3)	2.7141(17)
Ow(5)–H(51)	0.85(2)	Ow(7)	1.91(2)	171(2)	2.7603(17)
Ow(5)–H(52)	0.87(2)	O(4)	2.06(2)	167(3)	2.9143(16)
Ow(6)–H(61)	0.82(3)	Ow(7)	1.98(3)	167(3)	2.7847(18)
Ow(6)–H(62)	0.84(2)	Ow(5)	2.08(2)	169(2)	2.9099(16)
Ow(7)–H(71)	0.80(2)	Ow(2)	2.13(2)	160(3)	2.8991(16)
Ow(7)–H(72)	0.86(3)	O(1)	1.99(3)	161(3)	2.8203(19)

Table 8. Hydrogen-bond lengths (Å) and angles (°) for wilcoxite.

Donor (D)	D–H	Acceptor (A)	H...A	D–H...A angle	D...A
Ow(1)–H(11)	0.89(3)	Ow(11)	1.81(3)	177(5)	2.7008(13)
Ow(1)–H(12)	0.88(3)	Ow(11)	1.77(3)	170(4)	2.6389(13)
Ow(5)–H(51)	0.845(18)	Ow(11)	1.838(19)	174(2)	2.6790(13)
Ow(5)–H(52)	0.846(19)	O(1)	1.817(19)	176(2)	2.6617(14)
Ow(6)–H(61)	0.867(18)	O(3)	1.751(18)	176(2)	2.6169(13)
Ow(6)–H(62)	0.864(19)	Ow(12)	1.785(19)	175(2)	2.6472(14)
Ow(7)–H(71)	0.839(19)	O(2)	1.980(19)	175(2)	2.8166(14)
Ow(7)–H(72)	0.87(2)	Ow(10)	1.93(2)	175(2)	2.7973(15)
Ow(8)–H(81)	0.81(2)	O(2)	2.02(2)	168(2)	2.8143(15)
Ow(8)–H(82)	0.79(2)	Ow(10)	1.99(2)	175(2)	2.7772(16)
Ow(9)–H(91)	0.89(2)	O(2)	2.13(2)	177(2)	3.0200(15)
Ow(9)–H(92)	0.845(19)	Ow(12)	2.009(19)	173(2)	2.8492(16)
Ow(10)–H(101)	0.89(2)	O(4)	1.97(2)	169(2)	2.8546(15)
Ow(10)–H(102)	0.855(18)	O(1)	1.982(18)	166(2)	2.8201(14)
Ow(11)–H(111)	0.91(3)	F	1.76(3)	160(4)	2.6389(13)
Ow(11)–H(112)	0.91(3)	F	1.93(4)	142(4)	2.7008(13)
Ow(11)–H(113)	0.887(19)	O(4)	1.890(19)	163.2(19)	2.7510(14)
Ow(12)–H(121)	0.83(2)	O(3)	1.98(2)	174(2)	2.8018(14)
Ow(12)–H(122)	0.81(2)	O(4)	2.07(2)	173(2)	2.8798(15)

## ACKNOWLEDGMENTS

This research received support by MIUR through the SIR 2014 project “THALMIGEN – Thallium: Mineralogy, Geochemistry, and Environmental Hazards”, granted to CB. The constructive comments of S. Merlino and another anonymous reviewer are acknowledged.

## REFERENCES

- BACHET B., CESBRON F., CHEVALIER R., 1981. Structure cristalline de la khadémitte  $\text{Al}(\text{SO}_4)\text{F}\cdot 5\text{H}_2\text{O}$ . *Bulletin de Minéralogie* 104: 19-22.
- BAUR W.H., 1964. On the crystal chemistry of salt hydrates. IV. The refinement of the crystal structure of  $\text{MgSO}_4\cdot 7\text{H}_2\text{O}$  (epsomite). *Acta Crystallographica* 17: 1361-1369.
- BIAGIONI C., BONACCORSI E., ORLANDI P., 2011. Volaschioite,  $\text{Fe}^{3+}_4(\text{SO}_4)_2(\text{OH})_6\cdot 2\text{H}_2\text{O}$ , a new mineral species from Fornovolasco, Apuan Alps, Tuscany, Italy. *The Canadian Mineralogist* 49: 605-614.
- BRESE N.E., O'KEEFFE M., 1991. Bond-valence parameters for solids. *Acta Crystallographica* B47: 192-197.
- BROWN I.D., 1976. On the geometry of O–H...O hydrogen bonds. *Acta Crystallographica* A32: 24-31.
- BROWN I.D., ALTERMATT D., 1985. Bond-valence parameters obtained from a systematic analysis of the Inorganic Crystal Structure Database. *Acta Crystallographica* B41: 244-247.
- BRUKER AXS INC., 2004. Apex2. Bruker Advanced X-ray Solutions, Madison, Wisconsin, USA.
- CALLERI M., GAVETTI A., IVALDI G., RUBBO M., 1984. Synthetic epsomite,  $\text{MgSO}_4\cdot 7\text{H}_2\text{O}$ : absolute configuration and surface features on the complementary {111} forms. *Acta Crystallographica* B40: 218-222.
- CHOU I.-M., SEAL II R.R., 2007. Magnesium and calcium sulfate stabilities and the water budget of Mars. *Journal of Geophysical Research* 112: E11004.
- CIRIOTTI M.E., FERRERO S., BLASS G., AMBRINO P., 2008. Wilcoxite: primo ritrovamento italiano. *MICRO (UK report)* 2/2008: 75-76.
- DELAMÉTHÉRIE J.C., 1806. Tableau des analyses chimiques des minéraux, et d'une nouvelle classification de ces substances, fondée sur ces analyses. *Journal de Physique, de Chimie et d'Histoire Naturelle* 62: 319-365; 376-405.
- DYAR M.D., LANE M.D., BISHOP J.L., O'CONNOR V., CLOUTIS E., HIROI T., 2005. Integrated spectroscopic studies of hydrous sulfate minerals. *Lunar and Planetary Science* 36: 1622.
- FERRARIS G., IVALDI G., 1988. Bond valence vs bond length in O...O hydrogen bonds. *Acta Crystallographica* B44: 341-344.
- FERRARIS G., JONES D.W., YERKES J., 1973. Refinement of the crystal structure of magnesium sulphate heptahydrate (Epsomite) by neutron diffraction. *Journal of the Chemical Society Dalton Transactions* 1973: 816-821.
- FORTES A.D., WOOD I.G., ALFREDSSON M., VOČADLO L., KNIGHT K.S., 2006. The thermoelastic properties of  $\text{MgSO}_4\cdot 7\text{D}_2\text{O}$  (epsomite) from powder neutron diffraction and ab initio calculation. *European Journal of Mineralogy* 18: 449-462.
- HAWTHORNE F.C., KRIVOVICHEV S.V., BURNS P.C., 2000. The crystal chemistry of sulfate minerals. *Reviews in Mineralogy and Geochemistry* 40: 1-101.

- JAMBOR J.L., NORDSTROM D.K., ALPERS C.N., 2000. Metal-sulfate salts from sulfide mineral oxidation. *Reviews in Mineralogy and Geochemistry* 40: 303-350.
- JAMESON R., 1805. Natural Epsom salt. *System of Mineralogy*, II, Bell and Bradfute, Edinburgh, U.K., 22-24.
- KONG W.G., WANG A., FREEMAN J.J., SOBRON P., 2011. A comprehensive spectroscopic study of synthetic  $\text{Fe}^{2+}$ ,  $\text{Fe}^{3+}$ ,  $\text{Mg}^{2+}$ , and  $\text{Al}^{3+}$  copiapite by Raman, XRD, LIBS, MIR and vis-NIR. *Journal of Raman Spectroscopy* 42: 1120-1129.
- LOCKE A.J., MARTENS, W.N., FROST R.L., 2007. Natural halotrichites – an EDX and Raman spectroscopic study. *Journal of Raman Spectroscopy* 38: 1429-1435.
- MAJZLAN J., KIEFER B., 2006. An X-ray and neutron-diffraction study of synthetic ferricopiapite,  $\text{Fe}_{14/3}(\text{SO}_4)_6(\text{OD},\text{OH})_2(\text{D}_2\text{O}, \text{H}_2\text{O})_{20}$ , and *ab initio* calculations on the structure of magnesiocopiapite,  $\text{MgFe}_4(\text{SO}_4)_6(\text{OH})_2(\text{D}_2\text{O},\text{H}_2\text{O})_{20}$ . *The Canadian Mineralogist* 44: 1227-1237.
- MAJZLAN J., MICHALLIK R., 2007. The crystal structures, solid solutions and infrared spectra of copiapite-group minerals. *Mineralogical Magazine* 71: 553-569.
- MAURO D., BIAGIONI C., PASERO M., 2018a. Crystal-chemistry of sulfates from Apuan Alps (Tuscany, Italy). I. Crystal structure and hydrogen bond system of melanterite,  $\text{Fe}(\text{H}_2\text{O})_6(\text{SO}_4)\cdot\text{H}_2\text{O}$ . *Periodico di Mineralogia* 87: 89-96.
- MAURO D., BIAGIONI C., PASERO M., ZACCARINI F., 2018b. Crystal-chemistry of sulfates from Apuan Alps (Tuscany, Italy). II. Crystal structure and hydrogen bonding system of römerite,  $\text{Fe}^{2+}\text{Fe}^{3+}_2(\text{SO}_4)_4(\text{H}_2\text{O})_{14}$ . *Atti della Società Toscana di Scienze Naturali, Memorie, Serie A* 125: 5-11.
- ORLANDO T.M., McCORD T.B., GRIEVES G.A., 2005. The chemical nature of Europa's surface material and the relation to a subsurface ocean. *Icarus* 177: 528-533.
- PETERSON R.C., JOY B.R., 2013. Wilcoxite  $\text{MgAl}(\text{SO}_4)_2\cdot 17\text{H}_2\text{O}$ , from Rico, Colorado: occurrence and crystal structure. *The Canadian Mineralogist* 51: 107-117.
- QUARTIERI S., TRISCALI M., VIANI M., 2000. Crystal structure of the hydrated sulphate pickeringite ( $\text{MgAl}_2(\text{SO}_4)_4\cdot 22\text{H}_2\text{O}$ ): X-ray powder diffraction study. *European Journal of Mineralogy* 12: 1131-1138.
- SHANNON R.D., 1976. Revised effective ionic radii and systematic studies of interatomic distances in halides and chalcogenides. *Acta Crystallographica A* 32: 751-767.
- SHELDRIK G.M., 2015. Crystal structure refinement with SHELXL. *Acta Crystallographica C* 71: 3-8.
- VANIMAN D.T., BISH D.L., CHIPERA S.J., FIALIPS C.I., CAREY J.W., FELDMAN W.C., 2004. Magnesium sulphate salts and the history of water on Mars. *Nature* 431: 663-665.
- WANG A., FREEMAN J.J., JOLLIFF B.L., CHOU I-M., 2006. Sulfates on Mars: A systematic Raman spectroscopic study of hydration states of magnesium sulfates. *Geochimica et Cosmochimica Acta* 70: 6118-6135.
- WILLIAMS S.A., CESBRON F.P., 1983. Wilcoxite and lannonite, two new fluosulphates from Catron County, New Mexico. *Mineralogical Magazine* 47: 37-40.
- WILSON A.J.C. (editor), 1992. International Tables for Crystallography Volume C: Mathematical, Physical and Chemical Tables. Kluwer Academic Publishers, Dordrecht, The Netherlands.

(ms. pres. 2 maggio 2019; ult. bozze 13 giugno 2019)

Edizioni ETS

Palazzo Roncioni - Lungarno Mediceo, 16, I-56127 Pisa

[info@edizioniets.com](mailto:info@edizioniets.com) - [www.edizioniets.com](http://www.edizioniets.com)

Finito di stampare nel mese di dicembre 2019